*Toll, D.G., Md. Rahim, M.S., Karthikeyan, M. and Tsaparas, I. (2018) Soil atmosphere interactions for analysing slopes in tropical soils, Environmental Geotechnics https://doi.org/10.1680/jenge.15.00071.*

# Soil atmosphere interactions for analysing slopes in tropical soils

D.G. Toll, *BSc, PhD, DIC, Eur Ing, FICE, CEng*
*Professor, Department of Engineering, Durham University, UK*
*Email: d.g.toll@durham.ac.uk*

M.S. Md. Rahim, *BEng, MSc, PhD*
*Senior Geotechnical Engineer, Megaconsult Sdn. Bhd., Malaysia*

M. Karthikeyan, *BEng, MEng (Soil), MEng (Geotech), PhD*
*Senior Principal Engineer, Surbana Jurong Consultants Pte. Ltd, Singapore*

I. Tsaparas, *PhD, CEng, MICE*
*Associate Director, Benaim (An AECOM Company), Hong Kong*

**Keywords**
Landslides, Seepage, Finite-element modelling

**ABSTRACT:**

Modelling of soil-atmosphere interaction for slopes requires a proper understanding of the relevant soil parameters (soil water retention curve and the permeability function). This paper reports on numerical investigations of an instrumented residual soil slope in Singapore. The objective of the paper is to provide practical suggestions for choices of hydraulic parameters that can provide realistic predictions in analysing practical problems. The analyses use an uncoupled unsaturated flow model and a hydro-mechanical coupled model with time dependent boundary conditions. The results obtained using measured weather data for the slope were validated against field measurements of pore-water pressure changes. The models were able to capture the trend of changes in the pore-water pressure due to rainfall events provided account was taken of a more permeable surficial layer due to the presence of desiccation cracking and root passages. A comparative study of stability shows that the mobilised shear strength drops quickly during a rainfall event but recovers much more slowly during drying. This shows how

a series of regular rain storms with short periods of drying in between can cause a ratcheting effect, with rapid loss of strength during each period of rain that is not recovered during the intermediate drying periods..

## 1. **INTRODUCTION**

Modelling of weather effects on slopes in engineering practice increasingly makes use of finite element software to model the unsaturated flow aspects of the problem. This is commonly carried out using an uncoupled analysis, where flow modelling is used to produce pore-water pressure results that are then imported into a separate limit equilibrium slope stability analysis. In some cases a more sophisticated coupled analysis is performed, where the flow (hydrological) aspects and the geo-mechanical behaviour are both modelled using a finite element approach within a single software package, such that the equations for flow and mechanical response are solved together.

Unsaturated flow modelling requires a proper understanding of the relevant soil hydraulic parameters. These include the soil water retention curve (the relationship between soil suction and water content (or degree of saturation)) and the permeability function (that defines how the unsaturated permeability to water varies with suction). The objective of this paper is to consider practical measures for the choice of these parameters that can be used to provide realistic predictions. The choice of parameters is considered for a numerical investigation of a tropical residual soil slope at Nanyang Technological University (NTU) in Singapore, known as NTU Annex (NTU-ANX), to illustrate some key issues that need to be considered. The slope is an engineered slope in Jurong sedimentary formation residual soils.

The effects of desiccation cracking and vegetation on the hydraulic parameters are considered in this paper. These factors also influence the strength and erosion resistance of soils, through reinforcement or fissuring, but these aspects are not considered here. Only the effects on the development of suction and water content changes are considered. More detailed analyses of the modelling of vegetation have been reported by Indraratna et al., (2006), Rees and Ali (2006), Cui et al. (2013), Leung et al. (2015), Elia et al. (2017) and Tang et al. (2018). However, there has been less focus on the effect of desiccation cracking and root passages on the surficial permeability, which can often dominate the infiltration processes (Tsaparas and Toll, 2002).

The slope has been analysed using the finite element unsaturated flow model, SEEP/W, which is increasingly used in engineering practice. It is a commercial finite element code providing a two-dimensional, transient unsaturated seepage model. It can be used with SLOPE/W, a limit equilibrium slope stability analysis package that can import the pore water pressure data from SEEP/W in order to undertake stability analysis.

The case study has also been modelled using the PLAXIS finite element software which provides a coupled hydro-mechanical model. This is used to undertake evaluations of the mobilised shear strength (the shear strength available corresponding to the current pore-water pressure/suction state) and factor of safety of the slope as these change over time due to the actual rainfall data.

The paper also considers the differences of stability assessments between the two methods i.e. the limit equilibrium analysis using the Extended Mohr Coulomb ($\phi^b$) concept (Fredlund et al., 1978) in SLOPE/W and the finite element approach based on the application of the Bishop's stress concept (using $\chi$=Sr) (Schrefler, 1984) in PLAXIS.

## 2. HYDRAULIC PROPERTIES OF UNSATURATED SOILS

The soil water retention curve and the permeability function are both greatly affected by the heterogeneity of the subsurface soils due to fractures, fissures and cracks (Novak et al., 2000). The presence of open cracks and fissures can introduce a bi-modal form into the water retention function. Ignoring infiltration through these features usually leads to severely underestimated infiltration rates and hence an unrealistic description of the soil water regime (Van Genuchten et al., 1999). In vegetated slopes, root pathways and surface cracks can cause the coefficient of permeability to be significantly higher at the ground surface than at greater depths (Anderson et al., 1996).

It also needs to be recognized that these parameters change with time. As a soil dries out, desiccation cracks may appear and this will produce a major change in permeability. The macro permeability will also be highly anisotropic, as flow will be dominated by the secondary permeability of the crack system, which tends to form in a sub-vertical fashion. The water retention behaviour will also change as water can be held within the cracks. However, as swelling develops, the cracks may close and both permeability and water retention properties may change again. Chappell and Lancaster (2007) reported that the saturated coefficient of permeability to water ($k_{sat}$) values determined in a wet period were typically lower than the values determined in a dry period by up to a factor of two orders of magnitude.

Flow in structured porous media can be described using dual permeability models in which soil response consists of two regions, one associated with macro pores (the crack network) and the other with the less permeable matric region (Van Genuchten et al., 1999).

There are reports of laboratory measurements of the hydraulic properties of tropical residual soils from Singapore that are relevant to this case study. Agus et al. (2001) reported a large number of water retention curves for Singapore residual soil samples, at various depths. Soils near the ground surface might be expected to undergo more severe weathering compared to the underlying soils. However, Agus et al. (2001) examined the effect of weathering on the shape of the water retention curves and reported that there was no significant difference between the shape of these curves and the depth of weathering for the Jurong sedimentary formation residual soils. This suggests that the effect of surface cracking on the water retention function may not be as important as the major effects observed in permeability. Other measurements of water retention curves have been reported by Agus et al. (2003). They found that there was a similar trend in the shape of the water retention curve for the Jurong Sedimentary Formation residual soils even though there were differences in the saturated volumetric water content with depth.

Measurement of permeability functions for unsaturated soils are time consuming and there are often limited data. However, Agus et al. (2003; 2005) presented unsaturated permeability functions measured in the laboratory for Singapore residual soils. They show that the saturated permeability ($k_{sat}$) can vary between $10^{-10}$ m/s and $10^{-6}$ m/s. No clear trend was seen in the saturated coefficient of permeability with saturated volumetric water content, which highlights the difficulty of generalizing the properties of residual soils.

Because of the time-consuming nature of permeability measurements, it has become common to estimate the permeability function from the soil water retention curve (Fredlund et al., 1994). Integration functions for predicting the unsaturated permeability function from water retention data have been reported by Green and Corey (1971), Van Genuchten (1980) and Fredlund et

al. (1994), among others. It is important to recognise that there are dangers in using such expressions without an experimental confirmation of their validity, as will be discussed later.

An initial analysis of the case study in Singapore (NTU-ANX) was undertaken by Tsaparas and Toll (2002). They observed a discrepancy between the results of the numerical model and the field observations when considering the predicted infiltration. Using a field measured value of $k_{sat}=6x10^{-7}$ m/s and a Green and Corey (1971) derived permeability function, they showed that the numerical model predicted a total infiltration of 2.5 mm for a rainfall event on 23 March 2000, whereas the field measurements showed a total infiltration of 9 mm. The numerical model also predicted a low total infiltration of 8 mm for a rainfall event on 24 March 2000 whereas the field measurements showed a total infiltration of 15 mm.

Therefore, in order to achieve a closer match to the two sets of field observations from the NTU ANX slope (runoff/infiltration measurements and pore-water pressure measurements) in the numerical model, a more permeable layer, 0.25 m thick, was defined at the ground surface to model the vegetated and desiccated surficial zone of the slope. The depth of 0.25 m was based on the observed depth of root passages. It was found that a $k_{sat}$ value equal to $5x10^{-5}$ m/s for the surface material predicted total infiltration values that were in reasonable agreement with the field observations. For the rainfall event of 23 March 2000 the numerical model predicted a total infiltration equal to 7 mm (the field observation for this rainfall event was 9 mm total infiltration). For the rainfall event of 24 March 2000 the numerical model predicted a total infiltration of 17 mm (the field observation for this rainfall event was 15 mm).

Recognition of the presence of a more permeable surface layer produced predictions of total infiltration that were in agreement with the field observations and at the same time still gave pore-water pressure changes that were in reasonable agreement with the field measurements.

Rahardjo et al. (2013) have carried out a similar analysis for a case study in Singapore. They found that rainfall and evaporation in Singapore play equally important rôles in determining the flux boundary conditions of soil. The modelling of the evaporation process must be included for appropriate modelling of pore water pressure responses.

## 3. DESCRIPTION OF THE CASE STUDY

The case study under investigation was reported by Tsaparas et al. (2003). They presented data from an instrumented slope located on the campus of Nanyang Technological University (NTU), Singapore, where the Jurong sedimentary rock formation is the predominant geological formation. The NTU-ANX slope has an inclination of slope of 29°, height of 21m, and length of 43m. The ground surface of the NTU-ANX slope is covered with Buffalo Grass (*Brachiaria mutica*).

The simplified soil profile used in the two-dimensional, transient numerical modelling is illustrated in Figure 1. It consists of two soil layers. Layer 1 is the surface soil layer that extends to a depth of 10m. It is a hard silty to sandy clay that has an orange colour, moderate plasticity, and 58% fines. Layer 2 is clayey silt with siltstone and sandstone fragments and a fines content of 32%. The ground water table lies at depths between 15m and 17m from the ground surface and is not greatly affected by rainfall events. Hence, in this numerical analysis, the hydrological properties of soil layer 2 were less important and the same water retention curve as for Layer 1 has been used for this layer.

The main instrumentation of the NTU-ANX slope consisted of three rows of tensiometers, a rain gauge, and a piezometer. Three rows (A, B & C) of jet-fill tensiometers were spaced 3m apart (Figure 1). Each row consisted of five tensiometers (spaced 0.5m apart) for measuring the pore-water pressures at depths of 0.5, 1.1, 1.7, 2.3 and 2.9m. These measuring depths were chosen to study the variation of the pore pressure increase with depth during a rainfall event. The instrumented area of the site is relatively small (6m in length) in comparison with the size of the slope.

A rain gauge was installed next to the study area. The modelling of the case study focusses on the period from 23 March 2000 to 24 March 2000 (Tsaparas et al., 2003). During this time period two natural rainfall events were recorded on the slope. Figure 2 shows the recorded rainfall events from 23–24 March 2000 and the measured pore water pressure responses.

The pore-water pressures near the ground surface (at a depth of 0.5m) were most affected by the rainfall events and there was less significant change in the pore-water pressure profiles at greater depths. Md. Rahim and Toll (2014) have shown that the deeper responses (at 1.0m and below) can be captured well by numerical analyses, and for this paper only the responses at shallow depth of 0.5m will be reported.

It can be seen that the pore water pressure changes are small (2-3 kPa) and are close to the accuracy of field measurements. Although, the pressure transducers are capable of measuring to 0.1 kPa there could be variations of larger amounts due to temperature changes etc.. However, it can be seen that there are clear trends of responses that match with rainfall events that show that the measurements are reflecting real soil responses.

### 3.1 **Hydraulic Soil Properties used for the case study**

Figure 3(a) shows the water retention curve of a soil sample obtained from the NTU-ANX slope at a depth of 0.4m (Tsaparas, 2002). The saturated volumetric water content was 0.53 and when an applied suction of 200 kPa was established in the sample, the volumetric water content reduced to 0.38. This result in Figure 3(a) is compared with the envelope for water retention curves established for Jurong Sedimentary formation residual soils reported by Agus et al (2001) in Figure 3(b). The upper, average and lower water retention curves shown in Figure 3(b) were established using saturated volumetric water content of 0.53 and the curve fitting parameters reported in Agus et al. (2001).

Other water retention curves from the NTU campus reported by Agus et al. (2003) are also shown in Figure 3(b). These are for different depths (5.60m and 4.0m). The figure shows that there is similar trend in the shape of the water retention curve for the Jurong Sedimentary Formation residual soils even though there is difference in the saturated volumetric water content. The assessed versions of the soil hydraulic parameters adopted for the analysis are tabulated in Table 1.

In situ permeability measurements at the study area showed that the saturated coefficient of permeability, $k_{sat}$, for the surface soil is $6\times10^{-7}$ m/s, measured at approximately 0.4m deep using a Guelph Permeameter (Tsaparas et al., 2003). Other measurements for $k_{sat}$ of Jurong soil are given by Agus et al. (2003). They show that $k_{sat}$ can vary between $10^{-10}$ m/s and $10^{-6}$ m/s. The saturated volumetric water content for these soils varies between 0.25 and 0.60. No clear trend was seen in the saturated coefficient of permeability with saturated volumetric water

content. However, the field measurement by Tsaparas (2002) falls within the range of values, and is in agreement with data by Agus et al. (2003).

Figure 4 shows the unsaturated permeability functions measured for Jurong sedimentary formation residual soil samples based on data taken from Agus et al. (2003; 2005). From Figure 4, it can be seen that there is close agreement between the two soil samples (from different depths of 4.0m and 5.6m) for suctions above 20 kPa. Even though the saturated permeability values are different (due to differences in saturated volumetric water content as can be seen in Figure 3) the unsaturated permeability functions are almost identical in the higher suction range.

The commonly used integration functions for predicting the unsaturated permeability function from water retention data (Green and Corey, 1971; Fredlund et al. 1994; Van Genuchten, 1980) were investigated for the Jurong residual soil. The predicted curves showed significant differences between the experimental data reported by Agus et al. (2003) and the predictions. The Green and Corey (1971) method, based on the Tsaparas (2002) water retention curve shown in Fig. 3(b), gave a curve closest to the experimental results but was still very different (Fig. 4). This indicates the danger in using such expressions without an experimental confirmation of their validity.

It can be seen from Figure 4 that there is lack of information on experimental data near the air entry of value of the soil (below a matric suction of 20 kPa). Therefore, the Green and Corey (1971) equation was used to estimate the unsaturated coefficient of permeability values near the air entry of value up to the matric suction of 20 kPa using the water retention curve shown in Figure 3 with saturated coefficient of permeability of 6 x 10-7 m/s. The fitted Permeability

function shown in Figure 4 is based on the Green and Corey equation to 20 kPa suction and on experimental observations for higher suctions. This curve has been used in the analyses that follow.

For the surface desiccated upper part of Layer 1, the same saturated permeability value as used by Tsaparas and Toll (2002) of 5 x $10^{-5}$ m/s was adopted for the upper 0.25m, as indicated in Table 1.

### 3.2 **Shear Strength of Unsaturated Soils**

In SLOPE/W, the Extended Mohr-Coulomb concept (Fredlund et al., 1978) is used to carry out stability assessments for the residual soil slope. It is a concept that separates the contributions of net stress $(\sigma - u_a)$ and matric suction $(u_a - u_w)$ components as shown in Equation [1]:

$$\tau = c' + (\sigma - u_a) \tan \phi' + (u_a - u_w) \tan \phi^b \qquad [1]$$

where, $\tau$ = shear strength; $c'$ = effective cohesion for saturated condition; $\phi'$ = angle of shearing resistance for the saturated condition; $\phi^b$ = angle of shearing resistance with respect to matric suction for unsaturated conditions.

In the original formulation by Fredlund et al. (1978) the angle of shearing resistance for net stress was identified as $\phi^a$ and was later assumed to be equal to $\phi'$. This latter assumption may not always be the case (Delage et al., 1987, Toll, 2000, and Toll et al., 2008).

The strength parameters for the NTU-ANX site were measured by Gasmo et al. (1999) for Layer 1 and Layer 2 (Table 2). The parameters were obtained through saturated and unsaturated laboratory triaxial tests, providing the values of $\phi'$ and $\phi^b$ for the slope stability assessments considering unsaturated soil concepts. It is worth noting that for both layers, the values of $\phi'$

and $\phi^b$ were found to be equal for the range of suction investigated. This implies that that contributions from net stress and suction are equal, suggesting that an "effective stress" approach based on the assumption of saturation would be appropriate in this case.

In PLAXIS, the concept introduced by Bishop (1959) for "effective" stress in unsaturated soils is used for coupled analyses (Galavi, 2010).

$$\sigma' = \sigma - u_a + \chi\,(u_a - u_w) \qquad [1]$$

Where, $\sigma$, $\sigma'$ = the total and "effective" stress; $u_w$ = pore water pressure; $u_a$ = pore air pressure; $(\sigma - u_a)$ = net stress; and $(u_a - u_w)$ = matric suction and $\chi$ is a function of degree of saturation.

It has to be recognised that this simple concept of "effective stress" in unsaturated soils is not valid for all ranges of degree of saturation. It should not be seen as a true effective stress that controls all aspects of soil behaviour, as would be the case for saturated soils (Gens, 2010). However, it can provide a realistic approach at high degrees of saturation when the air phase is discontinuous.

This matric suction coefficient value ($\chi$), varies from 0 to 1, representing the condition of dry to fully saturated. Oberg and Sallfors (1997) and Vanapalli et al. (1996) recommended that the degree of saturation ($S_r$) or the effective degree of saturation ($S_e$) can be used as an approximate replacement for $\chi$. The effective degree of saturation ($S_e$) is used for $\chi$ in the PLAXIS formulation.

## 3.3 **Drying and evaporation**

The objective of the original numerical analyses was to study the seepage conditions of the NTU-ANX slope during infiltration. Therefore, the drying process of the slope between rainfall events was not the main focus of the study. However, it was necessary to incorporate drying into the analysis so that the numerical model could predict a realistic decrease of the pore water pressures during periods of no rainfall. Otherwise the initial values of pore-water pressure would be in error for rainfall events following a dry period.

During dry periods, the soil response should be modelled using the drying phase of the soil-water retention curve rather than the wetting curve. However, SEEP/W cannot handle hysteresis in these parameters, and the input functions have to be single curves. Therefore it was necessary for a switch between wetting and drying curves to be made by the user by changing the parameters at different time steps in the analysis. In initial analyses, the simulation was stopped immediately after the end of a rainfall event and the drying phase of the soil-water characteristic curve and permeability function was assigned for the surficial soil layer of the slope. The simulation then continued with these parameters until another rainfall event occurred, when the wetting curve was re-assigned.

The difficulty with this was the fact that after the end of a rainfall event, part of the slope (especially near the ground surface) starts to dry, while other parts of the slope (at greater depths) continue to wet due to percolation of water from above. However, it was not possible to overcome this, due to the limitations of SEEP/W. Nevertheless, it was interesting to see how the pore-water pressure changes were affected by using different wetting and drying curves. It was found that this has little effect on the decrease of the pore water pressures during the drying process. For this reason, it was decided to insert the drying phase of the soil-water

characteristic curve into the analysis only for dry periods that were longer than 12 hours. This methodology had the advantage that it allowed the study of the increase, during wetting, of the pore water pressures at large depths (where an increase in the pore-water pressures may occur long after the end of the rainfall event). In addition, possible numerical instabilities in the solution were reduced, as can occur when switching between different soil-water retention curves and permeability functions partway through an analysis.

To model drying, evapotranspiration had to be modelled as a negative (upward flux) over the whole slope surface within SEEP/W. The use of this methodology made it possible to predict the decrease of the pore-water pressures at all depths in a way that was comparable with the field measurements. The applied negative fluxes varied between $2.4 \times 10^{-10}$ m/s (i.e. 0.02 mm/day) and $5 \times 10^{-8}$ m/s (i.e. 4.3 mm/day). These values fall within the range of observed evaporation rates given by Gasmo et al. (2000).

### 3.4 **Effect of anisotropic permeability**

As noted earlier, the presence of cracking in the surficial layer is likely to induce significant anisotropy. This was modelled using a high permeability perpendicular to the surface (taking account of cracking and root passages in this direction), but maintaining the same value of permeability as the matrix soil for flow parallel to the ground surface. The ratio of hydraulic conductivities ($k_x/k_y$) was set to $1 \times 10^{-3}$, with the saturated value of $k_x$ set to $6 \times 10^{-7}$ m/s (and hence $k_y = 6 \times 10^{-4}$ m/s).

Figure 5 shows the comparison of the measured pore-water pressure in the field at a depth of 0.5 m (as reported in Figure 2) with the numerically predicted values when including the 0.25 m thick more permeable layer. The trend in the results is the same as that shown by the field

measured values. However, the numerical prediction still underestimates the magnitude of the pore water pressure change when compared with field measurement. Nevertheless they show improved predictions compared to the original analysis by Tsaparas and Toll (2002).

Further attempts have been made to introduce dual porosity and permeability models in the analysis. However, the numerical results show the inability of SEEP/W to handle the steep changes in material properties required; the solution tends to diverge instead of converge and oscillate between two extreme solutions represented by the extremities of the hydraulic conductivity function. This is a short coming that needs to be addressed by developing solvers that can ensure convergence under highly non-linear conditions (Fredlund, 2007).

## 4. **PLAXIS MODELLING**

Transient analyses were carried out using a fully coupled flow-deformation model by applying the Consolidation Total Pore Pressure (Consolidation-TPP) calculation option which is available in PLAXIS (Hamdhan and Schweiger, 2011). Hourly precipitation data, as shown in Fig. 2, was used as the flux boundary condition over the whole slope surface.

As PLAXIS only provides van Genuchten's (1980) equation for the permeability function, the curves created by Tsaparas and Toll (2002) (Figure 4) were refitted to gain equivalent van Genuchten parameters. The curves for wetting and drying are shown in Figure 6 (Md. Rahim and Toll, 2014). The curves shown are for the surface desiccated material with a saturated permeability of 5×10-5 m/s. The initial pore water pressure was taken as -3 kPa, based on the value used in Tsaparas and Toll's (2002) initial analysis.

Figure 7 shows a comparison of both the coupled (PLAXIS) and uncoupled (SEEP/W) analyses against the field data at 0.5m depth. Reasonable agreement can be seen between the two models. The models do explain the trends in fluctuations of pore-water pressures during rainfall; the curves show agreement with inclinations and declinations at the right time periods during and after rainfall events. This shows that the solutions are comparable.

Figure 7 shows the pore water pressures for the whole period 22-25 March 2000, with a 40 hours rain-free period before the rainstorm on 23rd March. It can also be seen that the starting pore water pressures of -3 kPa taken in the analysis of Tsaparas and Toll (2002) (based on a much longer time series analysis) is an underestimate of the true observed pore water pressure which drops from -1 to -2 kPa prior to the rain storm on 23 March. If an initial value of -1kPa were taken for the analysis, the curve would be shifted up by 2 kPa, and the agreement for the later pore water pressure would be much closer.

### 4.1 **Mobilised shear strength**

The stability analyses for the uncoupled SLOPE/W model uses the traditional limit equilibrium method. The Extended Mohr Coulomb concept incorporating $\phi^b$ is used to identify the mobilised shear strength ($\tau_m$) at the base of each slice in the analysis. The mobilised shear strength represents the shear strength available corresponding to the current pore-water pressure/suction state.

For the coupled analyses using PLAXIS, the principle of the shear strength reduction method (SSR) is used by simultaneously reducing $c'$ and $\phi'$ in small increments until a failure mechanism is created (Matsui and San, 1988). This stability assessment method, available in

many finite element codes, produces the concurrent reduction factor for the shear strength parameters and ultimately represents it as the factor of safety for the slope.

Figure 8 presents the correlation between mobilised shear strength ($\tau_m$) against the variations of pore-water pressure induced by rainfall. It is as anticipated that the $\tau_m$ value will decrease during both rainfall events as the increase in pore-water pressure consequently produces reduction in suction, weakening the soil.

It is interesting to note that during wetting a sharp increase in pore water pressure occurs that results in a rapid drop in mobilised shear strength (Figure 8). However, during the drying period following a rain storm, the pore water pressures drop much more slowly, so the resulting strength increase takes place quite gradually. Figure 9 shows a similar picture for degree of saturation, with rapid changes during wetting but taking longer to recover during drying. The more rapid response to wetting can be explained by the increase in pore water pressure (reduced suctions) induced by infiltration that will mean that flow into the surface is controlled by the saturated permeability. It can be seen from Fig. 4 that as the suction increases (as will occur during the drying phase) that the permeability reduces quickly, by one order of magnitude as suction increases to 2-3 kPa and by more than two orders of magnitude as suctions approach 10 kPa. Therefore, the drying phase will take longer to produce the same change in degree of saturation.

This shows how a series of regular rain storms with short periods of drying in between can cause a ratcheting effect, with rapid loss of strength during each period of rain that is not recovered during the intermediate drying periods.

The comparison between the stability assessments between the SLOPE/W uncoupled and the PLAXIS coupled model is shown in Figure 10. From the graph, it can be seen than the Factor of Safety (FOS) of the slope is slightly higher for the uncoupled analyses compared to the results for the latter. Although there is this difference in magnitude of FOS, which will be due to the different approaches of SSR and Limit Equilibrium methods (e.g. Aryal, 2008), the trends of the curves show a very similar shape as both FOS decline and rise up during and after rainfall infiltration.

## 5. **CONCLUSIONS**

Results are presented of numerical simulations of soil-atmosphere interaction of a tropical soil slope in Singapore using both uncoupled (SEEP/W) and coupled (PLAXIS) commercial finite element codes. The paper discusses the choices of input parameters for this type of modelling and provides practical suggestions for the choice of these parameters that can be used to provide realistic predictions. The results show that the prediction of changes in the pore-water pressure profile during precipitation and evapotranspiration is highly sensitive to the soil hydraulic properties used in the analysis. It was found that a SEEP/W uncoupled flow model was able to capture the general trend of field behaviour of the changes in the pore-water pressure profile due to rainfall events. This could only be achieved by taking account of a more permeable surficial layer to allow for the presence of desiccation cracking and root passages. Improved results could be achieved by recognising the anisotropy of permeability within the cracked zone.

The coupled PLAXIS code showed similar results for pore-water pressure responses using an unsaturated flow model and adopting the “Bishop stress” model for mechanical behaviour. The factor of safety determined for the slopes was compared between the shear strength reduction

method in the coupled model and the limit equilibrium method in the uncoupled model. The two models showed the same pattern of factor of safety reduction, although the limit equilibrium method gave slightly higher values, as has been found in other studies.

The results show that the mobilised shear strength drops quickly during a rainfall event but recovers much more slowly during drying. This shows how a series of regular rain storms with short periods of drying in between can cause a ratcheting effect, with rapid loss of strength during each period of rain that is not recovered during the intermediate drying periods. This rapid loss of strength during wetting and a slower recovery of strength during drying can be particularly important for tropical weather patterns, where regular (often daily) rainstorms occur, that can lead to a progressive loss of factor of safety if the drying periods are insufficiently long to allow strengths to recover between one storm and the next.

## REFERENCES


Agus, S.S., Leong, E.C. and Rahardjo, H. (2001) Soil-water characteristic curves of Singapore Residual soils. *Geotechnical and Geological Engineering*, 19, pp. 285-309.

Agus, S.S., Leong, E.C. and Rahardjo, H. (2003) A flexible wall permeameter for measurements of water and air coefficients of permeability of residual soils, *Canadian Geotechnical Journal*, 40, pp. 559-574.

Agus, S.S., Leong, E.C. and Rahardjo, H. (2005) Estimating permeability functions of Singapore residual soils, *Engineering Geology*, 78, pp. 119-133.

Anderson, M.G., Collison, A.J.C., Hartshorne, J., Lloyd, D.M. and Park, A. (1996) Developments in Slope Hydrology-Stability Modeling for Tropical Slopes, *Advances in Hillslope Processes*, Vol. 2, pp. 799-821.

Aryal, K.P. (2008). Differences between LE and FE Methods used in Slope Stability Evaluations, *Proc. 12th International Conference of International Association for Computer Methods and Advances in Geomechanics* (IACMAG), Goa, India, pp. 4509-4516.

Bishop A.W. (1959) The principle of effective stress, *Tecknisk Ukeblad*, 106 (39), pp 859-863.

Chappell, N.A and J. W. Lancaster, (2007) Comparison of methodological uncertainties within permeability measurements. *Hydrological Processes*, 21, pp. 2504-2514.

Cui, Y.J., Ta, A.N., Hemmati, S., Tang, A.M. Gatmiri, B. (2013) Experimental and numerical investigation of soil-atmosphere interaction, Engineering Geology 165, pp. 20-28.

Delage P., Suraj de Silva, G.P.R. and deLaure, E. (1987). Un nouvel appareil triaxial pour les sols non satures.. *Proc. 9th European Conf. Soil Mechanics and Foundation Engineering*, Dublin, Rotterdam: Balkema. 1, pp. 25-28

Elia, G., Cotecchia, F., Pedone, G., Vaunat, J., Vardon, P.J., Pereira, C., Springman, S.M., Rouainia, M., Van Esch, J., Koda, E., Josifovski, J., Nocilla, A., Askarinejad, A., Stirling, R., Helm, P., Lollino, P. and Osinski, P. (2017) Numerical modelling of slope–vegetation–atmosphere interaction: an overview, *Quarterly Journal of Engineering Geology and Hydrogeology*, 50, pp. 249–270.

Fredlund, D. G., Morgenstern, N.R. and Widger, R.A. (1978) The Shear Strength of Unsaturated Soils. *Canadian Geotechnical Journal*. 15, pp. 313-321.

Fredlund, D.G. (2007) Engineering Design protocols for unsaturated soils. *Proc. 3rd Asian Conference on Unsaturated Soils*, edited by Yin, Z., Yuan, Z and Chiu, A.C.F. Science Press, Beijing, China, pp. 27-45.

Fredlund, D.G., Xing, A. and Huang, S. (1994) Predicting the permeability functions for unsaturated soils using the soil-water characteristics curve, *Canadian Geotechnical Journal*, 31, pp. 533-546.

Galavi, V. (2010) Groundwater flow, fully coupled flow deformation and undrained analysis in PLAXIS 2D and 3D, *Plaxis Report*, http://kb.plaxis.nl/ .

Gasmo J.M, Hritzuk K.J., Rahardjo H. & Leong E.C. (1999) Instrumentation of an Unsaturated Residual Soil Slope. *Geotechnical Testing Journal*, 22, pp. 128-137

Gasmo J.M, Rahardjo H. & Leong E.C. (2000) Infiltration effects on stability of a residual soil slope. *Computers and Geotechnics*. 26, pp. 145-165.

Gens A. (2010) Soil environment interactions in geotechnical engineering. *Géotechnique*, 60 (1), pp. 3-74.

Green, R.E. and Corey, J. C. (1971). Calculation of hydraulic conductivity: A further evaluation of some predictive methods, *Proc. Soil Science Society of America*, 35, pp. 3-8.

Hamdhan I.N. and Schweiger F.H. (2011) Slope Stability Analysis of Unsaturated Soil with Fully Coupled Flow-Deformation Analysis. *IAMG 2011*, Salzburg, Austria.

Indraratna, B., Fatahi, B., & Khabbaz, H. (2006). Numerical analysis of matric suction effects of tree roots. *Geotechnical Engineering - Proc. Institution of Civil Engineers*, 159, pp. 77-90.

Leung, A. K., Garg, A., & Ng, C. W. W. (2015). Effects of plant roots on soil-water retention and induced suction in vegetated soil. *Engineering Geology*, 193, pp. 183-197.

Matsui T. and San K.C. (1988). Finite element stability analysis method for reinforced slope cutting. *Proc. Int. Geotechnical Symposium on Theory and Practice of Earth Reinforcement*, Fukuoka, Japan. pp.317–322.

Md. Rahim, M.S. and Toll D.G. (2014) Fully Coupled Flow-Deformation Analyses of Infiltration and Matric Suctions within a Tropical Soil Slope. in *Unsaturated Soils: Research & Applications*, (Eds. N. Khalili, A. Russell & A. Khoshghalb), London: Taylor & Francis (CRC Press).

Novak, V., Simunek, J. and Genuchten, M.Th. (2000). Infiltration of water into soil with cracks. *Journal of irrigation and Drainage Engineering*, 126 (1), pp.41-47.

Oberg, A. and Sallfors, G. (1997). Determination of shear strength parameters of unsaturated silts and sands based on the water retention curve, Geotechnical Testing Journal, GTJODJ 20(1): p. 40–48.

Rahardjo, H., Satyanaga, A. and Leong, E.C. (2013) Effects of flux boundary conditions on pore-water pressure distribution in slope, *Engineering Geology* 165, pp. 133-142.

Rees, S. W., & Ali, N. (2006). Seasonal water uptake near trees: a numerical and experimental study. *Geomechanics and Geoengineering: An International Journal*, 1(2), pp. 129-138.

Schrefler, B. (1984) *The finite element method in soil consolidation (with applications to surface subsidence).* PhD thesis, University College Swansea.

Tang, A-M., Hughes, P., Dijkstra, T., Askarinejad, A., Brencic, M., Cui, Y-J., Diez, J.J., Firgi, T., Gajewska, B., Gentile, F., Grossi, G., Jommi, C., Kehagia, F., Koda, E., ter Maat, H.W., Lenart, S., Lourenco, S., Oliveira, M., Osinski, P., Springman, S.M., Stirling, R., Toll, D.G. and van Beek, V. (2018). Atmosphere - vegetation - soil interactions in a climate change context; changing conditions impacting on engineered transport infrastructure slopes in Europe. Accepted for *Quarterly Journal of Engineering Geology and Hydrogeology*.

Toll, D.G. (2000). The influence of fabric on the shear behaviour of unsaturated compacted soils. *Advances in Unsaturated Soils, Geotechnical Special Publication No.99* (eds. Shackleford, C., Houston, S.L. and Chang, N.Y.), Reston American Society of Civil Engineer. pp. 222-234.

Toll, D.G., Ali Rahman, Z. & Gallipoli, D. (2008). Critical state conditions for an unsaturated artificially bonded soil, *Unsaturated Soils: Advances in Geo-Engineering*. Proc. 1st European Conf. Unsaturated Soils, Durham (eds. Toll, D.G., Augarde, C.E, Gallipoli, D. and Wheeler S.J.) Leiden: CRC Press/Balkema. pp. 435-440.

Tsaparas, I. (2002). *Field measurements and numerical modeling of infiltration and matric suctions within slopes*, PhD Thesis, School of Engineering, Durham University. 314p. (available online: http://etheses.dur.ac.uk/1715/)

Tsaparas, I. and Toll, D.G. (2002) Numerical Analysis of Infiltration into Unsaturated Residual Soil Slopes. *Proc. 3rd International Conference on Unsaturated Soils, Recife, Brazil, Lisse: Swets & Zeitlinger.* 2, pp. 755-762.

Tsaparas, I., Rahardjo, H., Toll, D.G. & Leong, E.C. (2003) Infiltration Characteristics of Two Instrumented Residual Soil Slopes, *Canadian Geotechnical Journal*, 40(5), pp. 1012-1032.

Van Genuchten, M.T. (1980). A closed-form equation for predicting the hydraulic conductivity of unsaturated soils. *Soil Science Society of America Journal*, 44, pp. 892-898.

Van Genuchten, M.T., Schaap, M.G., Mohanty, B.P. Simunek, J and F.J. Leij (1999). Modeling flow and transport processes at the local scale, in *Modeling of transport process in soils at various scales*, J.Feyen and K. Wiyo (eds.), Wageningen, The Netherlands, pp. 23-45.

Vanapalli, S.K., Fredlund, D.G., Pufahl, D.E., and Clifton, A.W. (1996). Model for the prediction of shear strength with respect to soil suction. *Canadian Geotechnical Journal*, 33: 379-392.

Table 1. The hydraulic parameters for each soil layer of the slope

| Soil Layer | Description | $k_{sat}$ (m/s) | Van Genuchten parameters for the water retention curves | | | | | |
|---|---|---|---|---|---|---|---|---|
| | | | Wetting | | | Drying | | |
| | | | a | m | n | a | m | n |
| 1 | Silty to sandy CLAY | $6\times10^{-7}$ (*) | 3.36 | 0.319 | 1.47 | 3.30 | 0.075 | 1.08 |
| 2 | Clayey SILT with siltstone and sandstone | $6\times10^{-8}$ | 3.36 | 0.319 | 1.47 | 3.30 | 0.075 | 1.08 |

* For the surface desiccated upper part of the layer, a value of $k_{sat}=5\times10^{-5}$ m/s was adopted.

Table 2. The strength parameters for each soil layer of the slope (Gasmo et al., 1999).

| Soil Layer | Friction angle, $\phi'$ (°) | Friction angle, $\varphi^b$(°) | Cohesion, $c'$ (kPa) | Unit weight | |
|---|---|---|---|---|---|
| | | | | $\gamma$ (kN/m$^3$) | $\gamma_{sat}$ (kN/m$^3$) |
| 1 | 30 | 30 | 1.2 | 19 | 20 |
| 2 | 31 | 31 | 1.4 | 19 | 20 |

## Figures

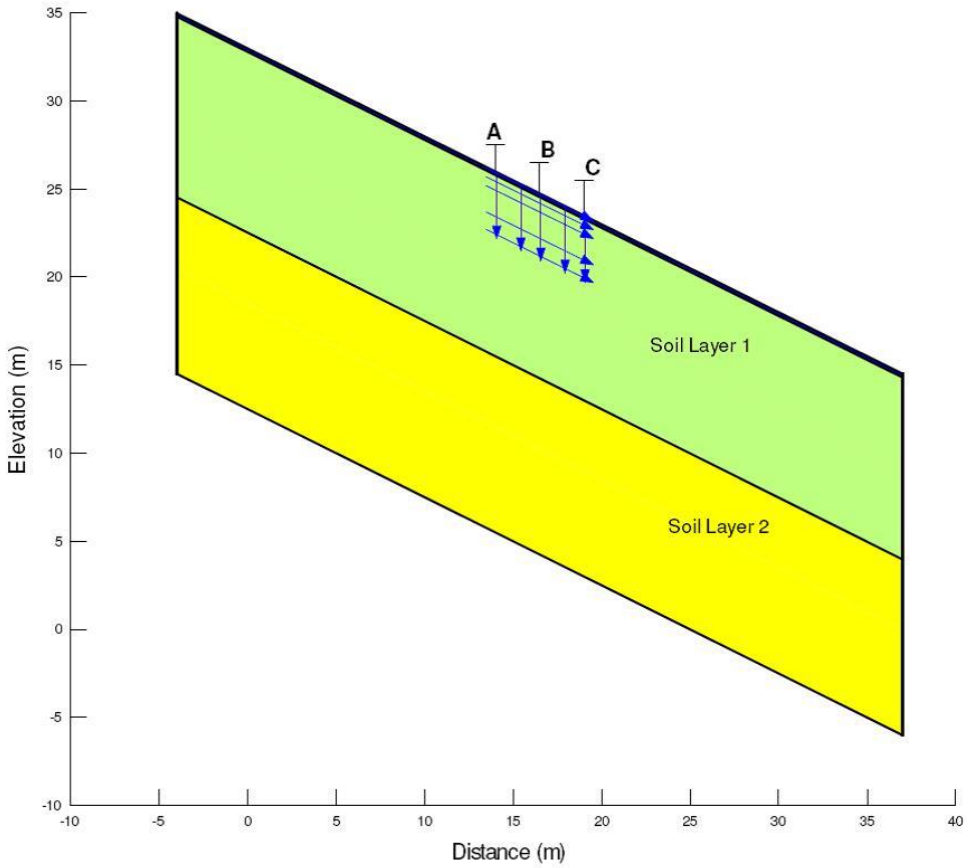


Figure 1. Geometry of the slope used in the numerical analysis

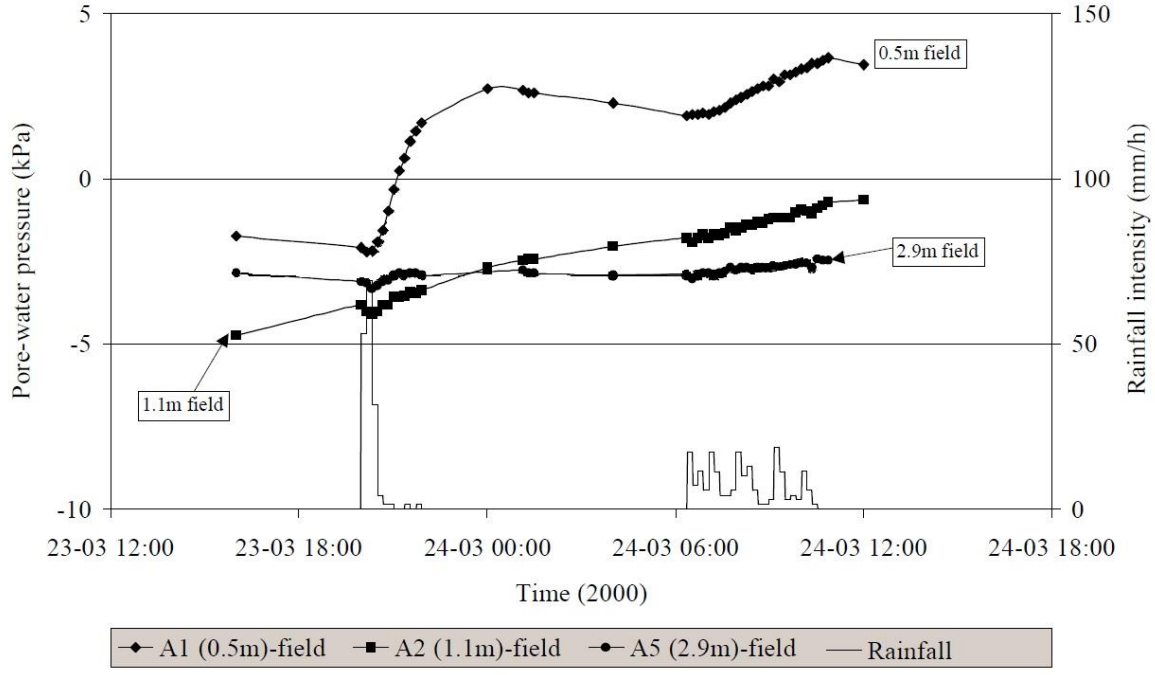


Figure 2. Recorded rainfall events from 23 - 24 March 2000 and recorded pore water pressures at depths of 0.5m, 1.1m and 2.9m.

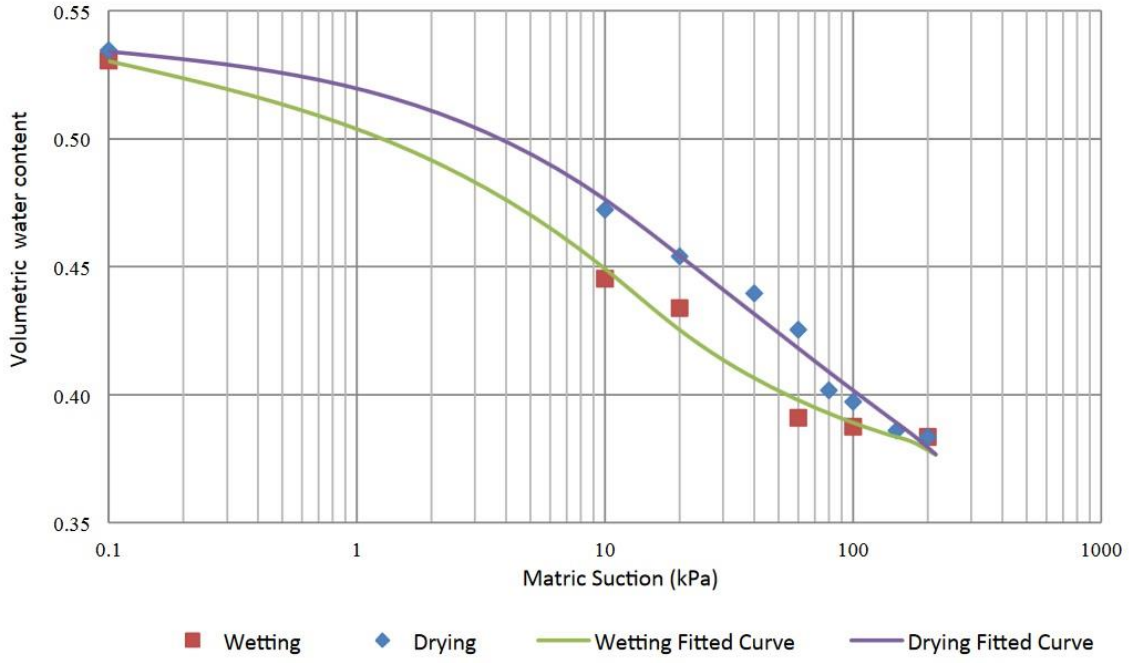


(a)

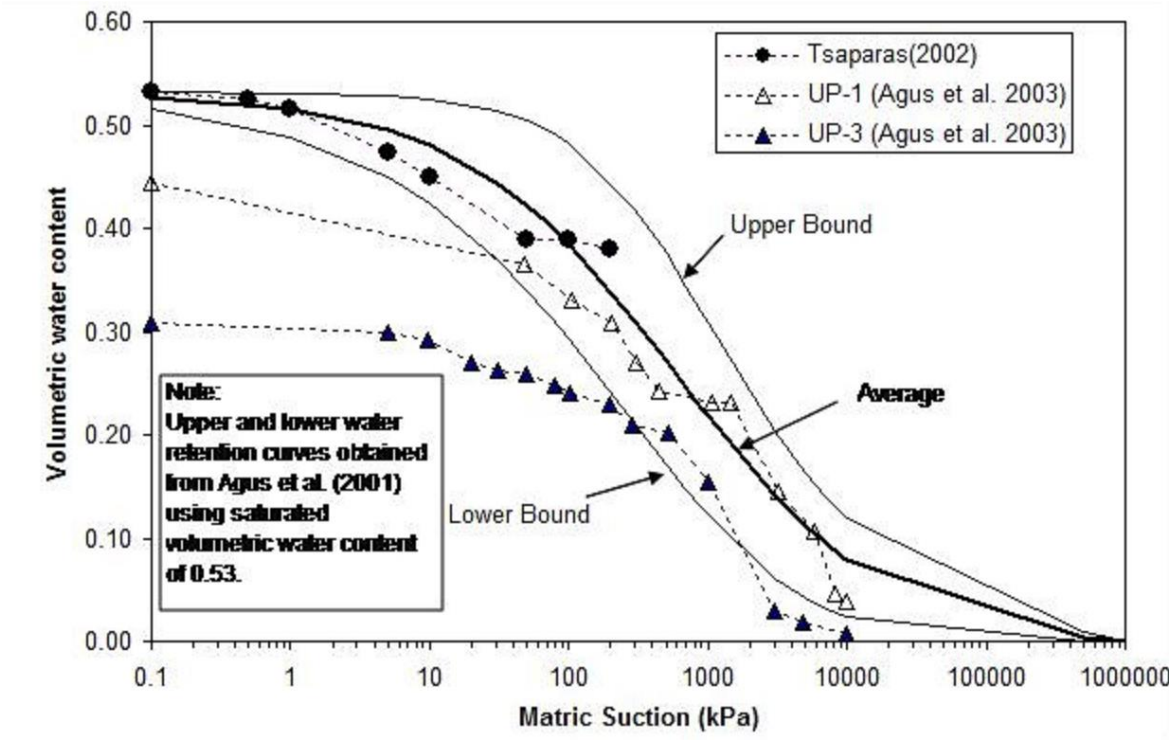


(b)

Figure 3. Water retention curve envelopes for Jurong formation residual soils (a) measured by Tsaparas (2002) (b) compared with data from Agus (2001; 2003). (UP-1 corresponds to a depth of 4.0m and UP-3 to a depth of 5.6m).

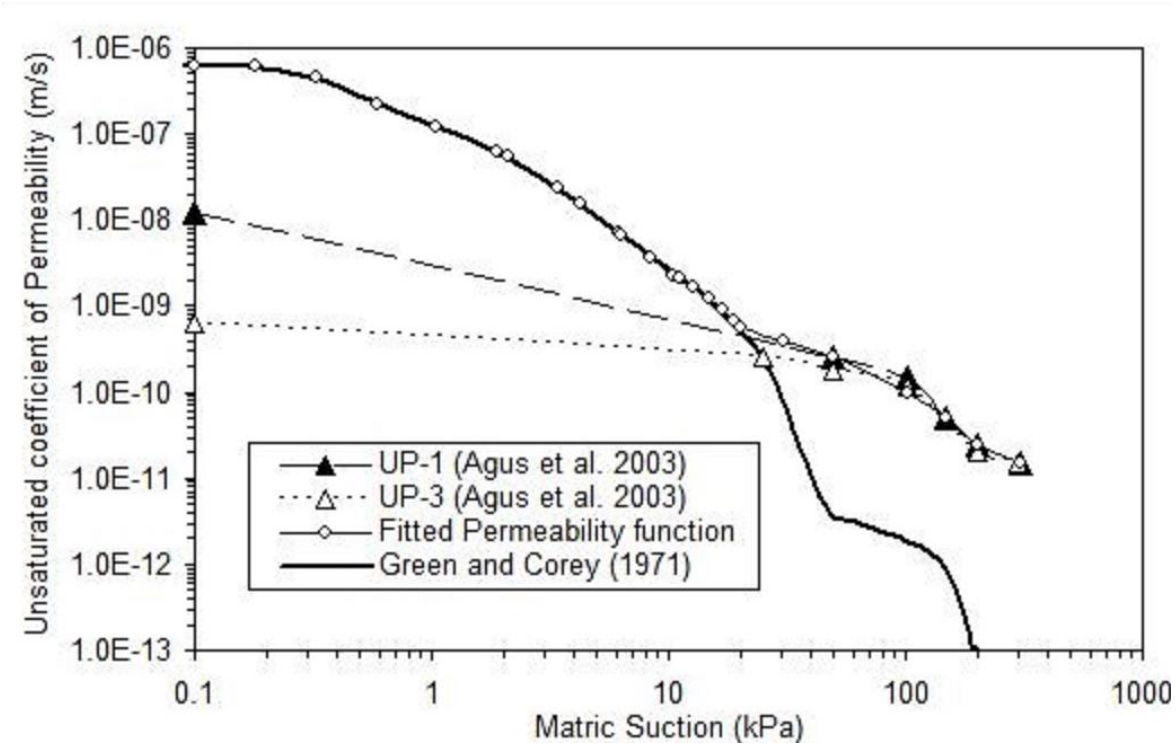


Figure 4. Measured unsaturated permeability function for Jurong Sedimentary Formation (UP-1 corresponds to a depth of 4.0m and UP-3 to a depth of 5.6m).

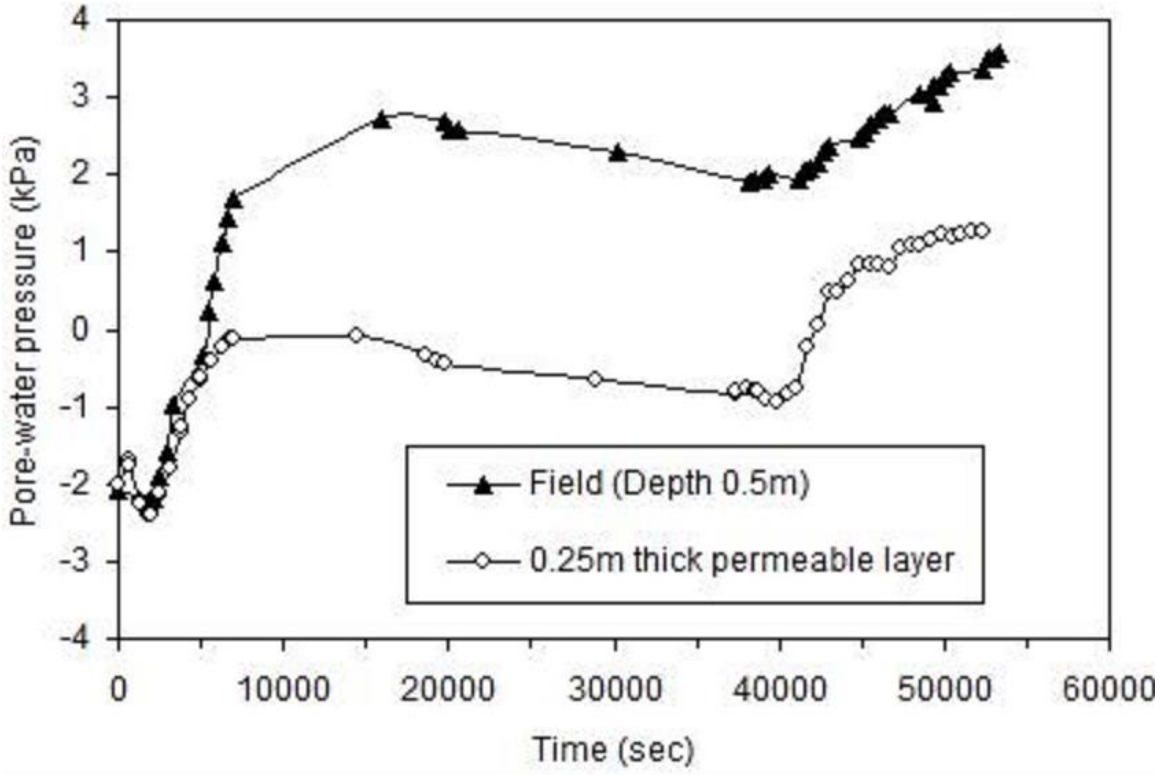

Figure 5. Comparison of pore water pressure variations for an anisotropic surficial layer

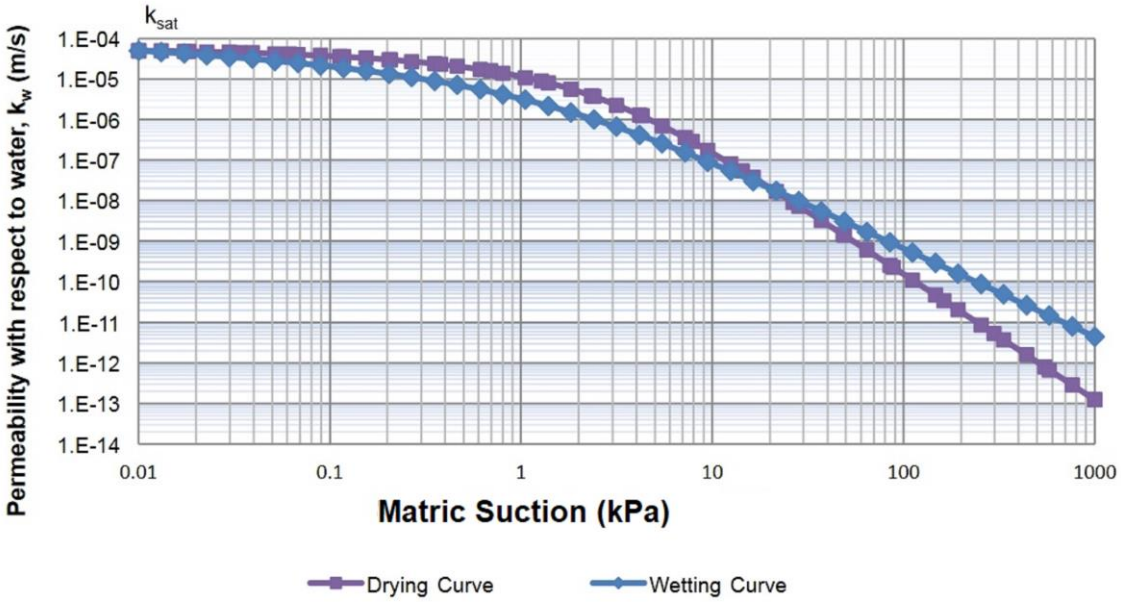


Figure 6. Permeability Functions using van Genuchten (1980)

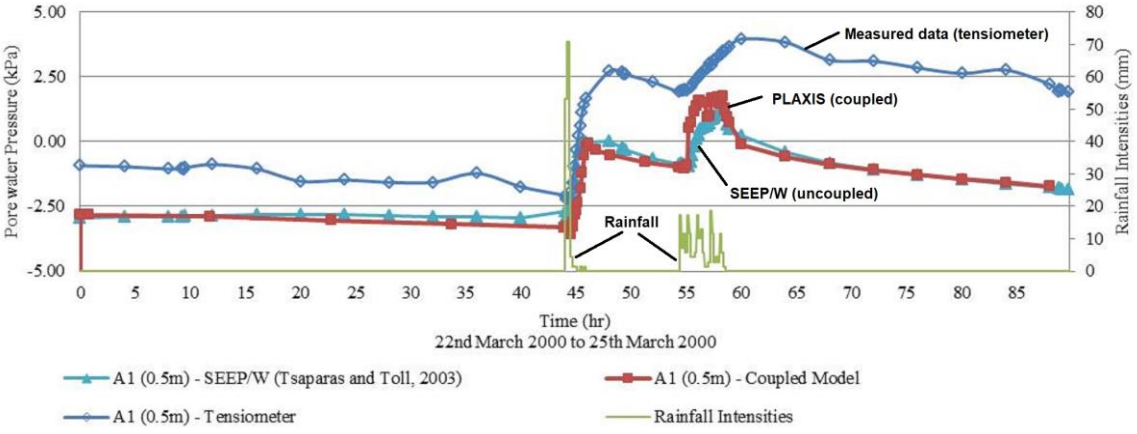


Figure 7. Comparison on SEEP/W and PLAXIS analyses at a depth of 0.5m.

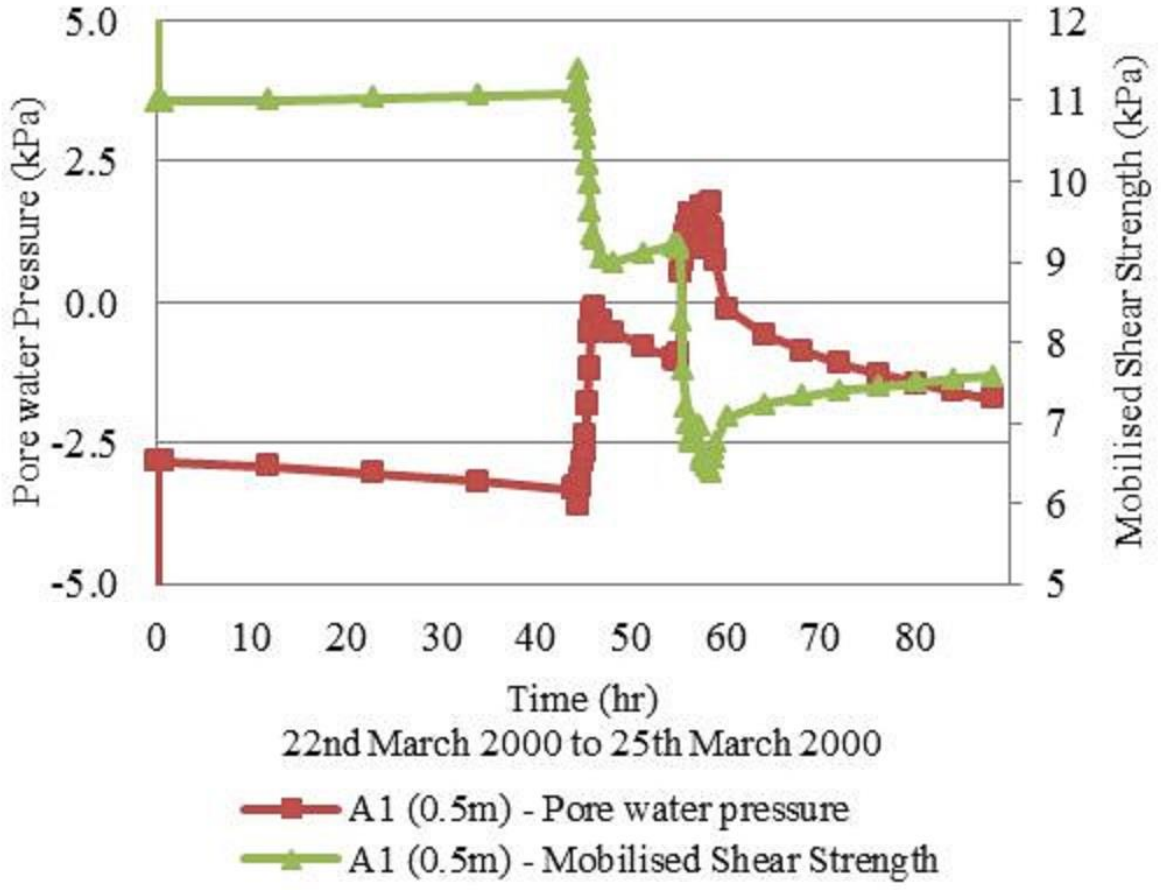


Figure 8. Pore water pressure and mobilised shear strength at 0.5m of NTU-ANX from 23rd March to 24th March 2000.

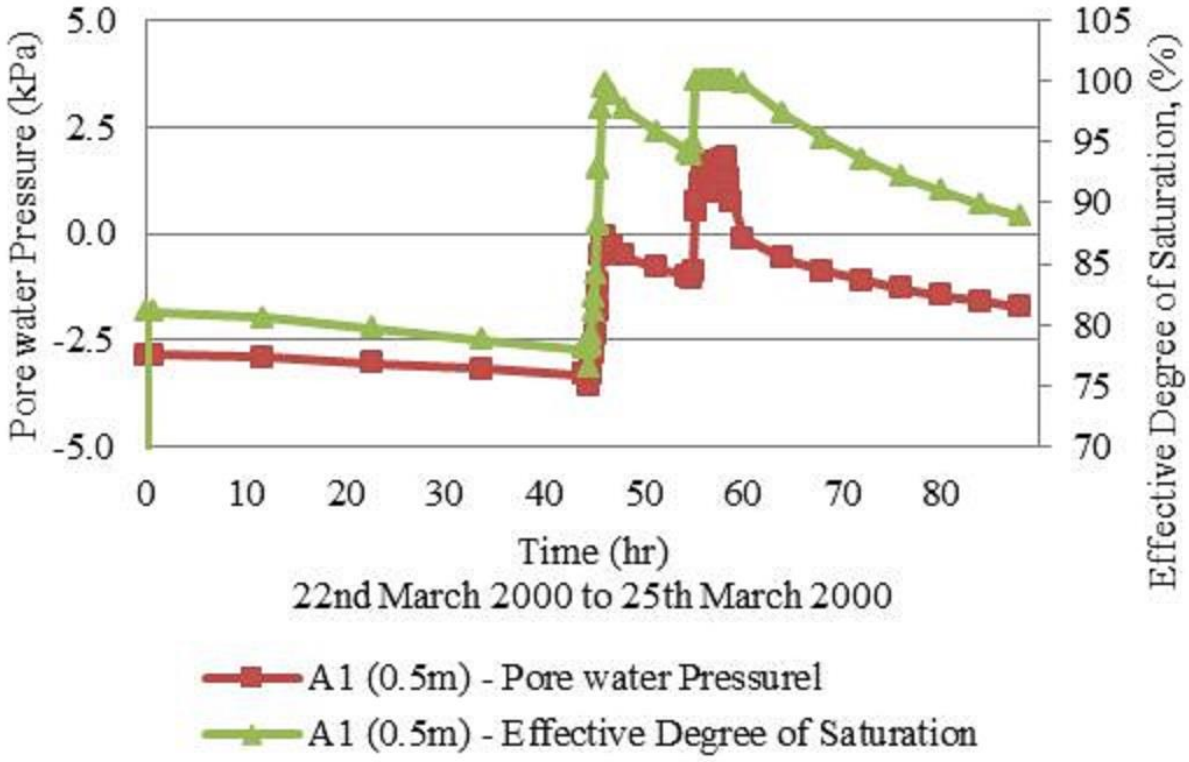


Figure 9. Pore water pressure and degree of saturation at 0.5m of NTU-ANX from 23rd March to 24th March 2000.

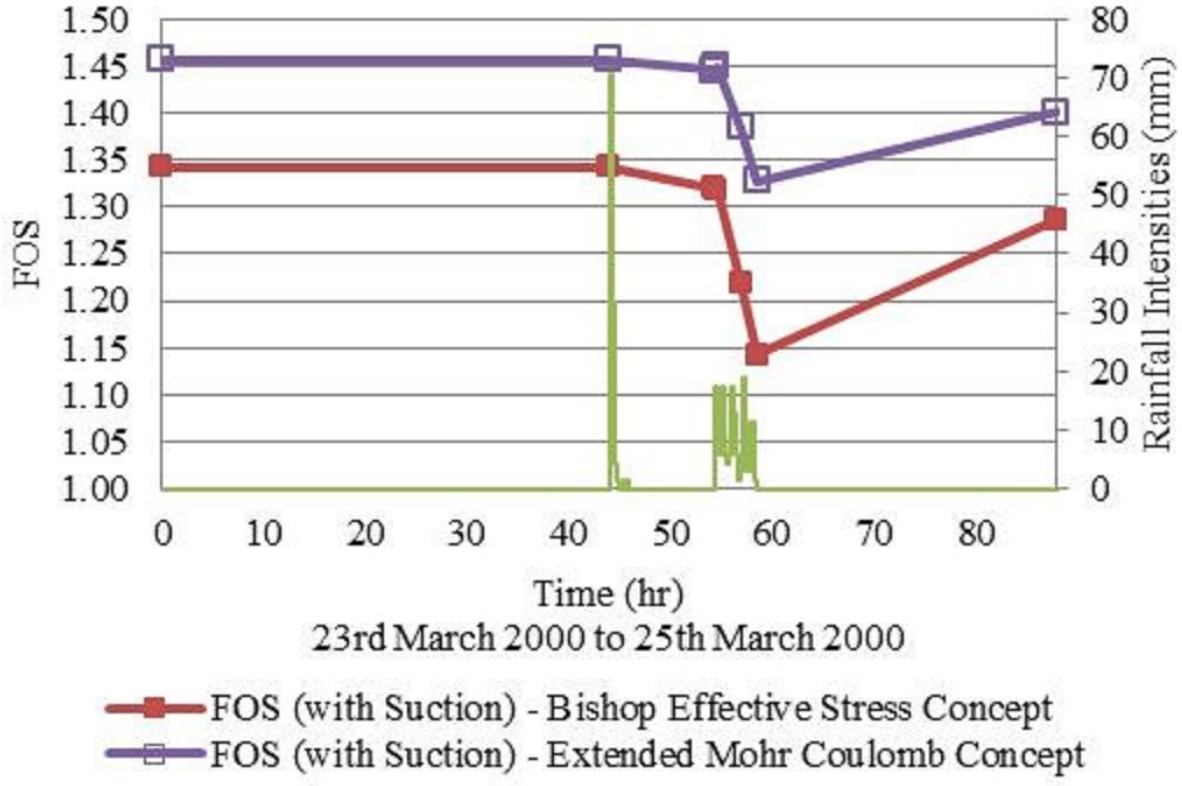


Figure 10. Factor of safety value against time from 23rd March to 24th March 2000.